2014 年 8 月
碩士學位論文

히트파이프와 U자 관을 이용한 진공관형 태양열 집열기의 열전달 성능에 대한 해석

朝鮮大學校 大學院

機 械 工 學 科

童 逸 杰

히트파이프와 U자 관을 이용한 진공관형 태양열 집열기의 열전달 성능에 대한 해석

Theoretical and experimental analysis on the thermal performance of evacuated solar collector with heat pipe and U tube

2014年 8月 25日

朝鮮大學校 大學院

機 械 工 學 科

童 逸 杰

히트파이프와 U자 관을 이용한 진공관형 태양열 집열기의 열전달 성능에 대한 해석

指導敎授 : 曺 弘 鉉

이 논문을 공학석사 학위신청 논문으로 제출함

2014 年 4 月

朝鮮大學校 大學院

機 械 工 學 科

童 逸 杰

童 逸 杰의 碩士學位 論文을 認准함

委員長 朝鮮大學校 敎 授 洪 明 錫 ㊞

委 員 朝鮮大學校 敎 授 金 志 勳 ㊞

委 員 朝鮮大學校 敎 授 曺 弘 鉉 ㊞

2014 年 5 月

朝鮮大學校 大學院

Contents

List of Figures

List of Tables

Nomenclature

A	: area (m^2)
C_p	: heat capacity (J/kg K)
D	: diameter (m)
ESCHP	: evacuated solar collector of heat pipe (-)
ESCU	: evacuated solar collector of U-tube (-)
F	: fin efficiency of straight fin (-)
F_a	: solar collector efficiency factor for ESCHP (-)
F'	: solar collector efficiency factor for ESCU (-)
G	: solar radiation (W/m^2)
h	: heat transfer coefficient (W/m^2K)
h_{ga}	: convection heat transfer coefficient from the outer glass tube to the surroundings (W/m^2K)
h_{pgd}	: heat transfer coefficient through conductivity between the absorber tube and the glass tube (W/m^2 K)
h_{pgc}	: radiation heat transfer coefficient between the absorber tube and the glass tube (W/m^2K)
I	: absorbed solar radiation by absorber coating, (W/m^2)
k	: conductivity, W/(K m)
L	: length (m)
m	: flow rate (kg/s)
Nu	: Nusselt number (-)
Pr	: Prandtl number (-)
Q	: heat (W)

Q_L : thermal loss (W)

Q_u : net heat gained by the working fluid (W)

R : thermal resistance (K/W)

Re : Reynolds number (-)

r : radius (m)

T : temperature (K)

t : thickness (m)

U : heat loss coefficient (W/m^2K)

U_{edge} : edge loss coefficient of the header tube (W/m^2K)

Greeks

η : efficiency (-)

ε : emissivity (-)

$\tau\ \alpha$: transmission-absorbance coefficient (-)

ϕ : nanoparticles volume concentration (-)

Subscripts

a : ambient (-)

b : bond (-)

bf : base fluid (-)

bulk : bulk material (-)

c : absorber tube (-)

con : condenser (-)

com : component (-)

evap : evaporator (-)

f : fluid (-)

fu : fluid and U-tube wall (-)

g : glass tube (-)

hp : heat pipe (-)

I : inlet, inside (-)

lv : liquid-vapor interfaces (-)

nf : nanofluid (-)

o : outlet (-)

p : pipe (-)

s : synthetic/solid particle (-)

t : tube (-)

u : useful (-)

v : vapor (-)

w : wick (-)

초록

히트파이프와 U자 관을 이용한 진공관형 태양열 집열기의 열전달 성능에 대한 해석

동 역 걸
지도교수: 조 홍 현
조선대학교 기계공학과 대학원

실험을 통한 태양열 집열기의 열성능에 대한 많은 연구가 수행되었다. 본 연구에서는 태양복사로부터 발생하는 열을 이용하여 상대적으로 높은 효율을 얻을 수 있는 U-Tube(ESCU)를 채용한 진공형 태양열 집열기와 히트파이프(ESCHP)를 설계하였다.두 집열기의 열성능은 처음으로 연구되었고 결과는 아래와 같다. 비교내용에 있어 두 태양열 집열기의 종류에 대한 시뮬레이션과 실험 결과는 상당한 일치를 보인다. 두 모델에 있어 맑은 날에는 히트파이프가 U-Tube에 비해 약 10%정도 높은 효율을 가지지만 흐린 날의 경우 U-tube가 히트파이프에 비해 더 일정하며 더 좋은 열성을 가지는 효율의 불일치성을 가진다. 매니폴드 내의 물 대신에 태양열집열기에 나노유체를 적용 할 경우, MWCNT 나노유체는 모 유체에 비해 높은 열물성치를 가지기 때문에 작동유체로써 좋은 선택이다. 그리고 구리 핀과 U-tube 태양열 집열기 사이의 종합적 전도의 영향성을 연구하였다. 0.24 vol%인 나노유체는 작동유체와 관 사이에서의 열전달계수가 상대적으로 높았으며 물보다 8% 높은 결과를 보였다. 또한 전도가 물성치의 인가인 0.17 W/m·K 보다 클 경우, 이에 대한 결과는 무시할 수 있다.

I. Introduction

A. Background

It is universally acknowledged that energy pollution is becoming more and more serious around the world. For sustainable development and the world environment, the applications of solar energy to electricity generation and heat collection have become important, and have attracted global attention by the study of Hottel(1942) and Grag(1975). The power source of the sun is absolutely free and the production of solar energy produces no pollution. As a result, technological advancements have made solar energy systems extremely cost-effective. Most systems do not require any maintenance during their lifespan, which means never having to invest money into them again. Furthermore, unlike traditional large-scale panel systems, many modern systems are sleeker, such as Uni-Solar rolls that lay directly on the roof like regular roofing materials. Solar energy systems are now also designed for particular needs. In Korea, solar collectors are widely used for building heating or heat systems because of their good thermal performance.

However, a great deal of research has been done to improve the thermal performance of solar collectors. The power of the Sun is absolutely free, and the production of solar energy does not pollute the environment. As a result, technological advancements have made solar energy systems extremely cost-effective. Take China, for instance. Currently, nearly three-quarters of its electricity is generated by coal-fired power plants. However, its rich solar resources are expected to be fully utilized to reduce greenhouse gas emissions, and Wang(2010) reported

several large-scale parabolic trough solar fields (supported by the Chinese Ministry of Science and Technology) are under construction. Most systems do not require any maintenance during their lifespan, which means never having to invest money in them. Furthermore, unlike traditional large-scale panel systems, most modern systems, such as Uni-Solar rolls, are sleek since they lay directly on the roof like regular roofing materials. Solar energy systems are now also designed for specific needs.

With resource shortages, the utilization of new energy has become a necessity for sustainable development. In the last century alone, many countries have studied and employed solar collectors, using them in the design of buildings. The solar collector has gradually come into use by the general public as well. As a result, the technology for the utilization of solar energy has rapidly developed in recent years, and competitiveness with conventional energy has been achieved. Solar collectors transform solar radiation into thermal energy. Heat pipes are devices with high thermal conductance that can transfer energy through the two-phase circulation of a fluid and a gas, which can be easily integrated into most collectors. Solar energy also has advantages and disadvantages in terms of cost, lack of pollution, and custom design for particular needs. It is estimated that the world's oil reserves will last for 30 to 40 years, whereas solar energy is practically infinite. However, solar energy can only be harnessed in the daytime when it is sunny, so in countries such as the UK, an unreliable climate means that solar energy is an unreliable source of energy. Cloudy skies can reduce the effectiveness of such an energy source, and large areas of land are required to collect useful energy from the Sun. Collectors are usually arranged together, especially when electricity is to be produced and used in the same location. Various

works have studied solar insolation and provided precise equations to predict the thermal efficiency of solar collectors.

Solar collector as a solar energy recovery device recovers the energy of sun and converts it to heat. It includes solar water heater and solar air heater that produce hot water and air respectively. It can be stated that solar collectors convert solar radiation into heat. Solar radiation, which includes high amount of energy, can conduct the energy of the sun through photons to the fluid. It has been shown by Kalogirou(2004) that solar collectors have a significant role in reducing energy consumption. Moreover, the use of nanoparticles within the working fluids (nanofluids) permits to enhance the heat transfer, therefore increasing the thermal performance of the collector. Sani(2010) found that nanofluid (liquid nanocomposite) is a mixture of a liquid substance (basefluid) and nanometer-sized material (nanoparticle). Nano-science has a very important role in promoting technology in HVAC and equipment field.

Previously, low-concentration solar thermal systems have been developed and analyzed for a long term. The CPC collector was invented and presented by Winston(1974). The solar collector in this study has eight concentric evacuated tube collectors, which can be reliably operated for getting heat for residential applications. And for working fluid, MWCNT is chose because of its good thermal character. Natarajan and Sathish(2009) investigated the thermal conductivity improvement of base fluids employing carbon nanotube (CNT) and recommended if these fluids were used as a heat transport medium, it could raise the efficiency of the traditional solar water heater.

There are several types of solar collectors: U-tube-type, flat-plate-type, and heat-pipe-type. Heat pipe evacuated tubular solar collectors have advantages such

as anti-freezing, rapid start-up, resistance to high pressure, and easy installation and maintenance, and several countries have been paying more attention to them. A feature that makes heat pipes attractive for use in solar collectors is their ability to operate like a thermal diode in that the flow of heat is in one direction only. This minimizes heat loss from the transporting fluid (e.g., water) when incident radiation is low. Furthermore, when the maximum design temperature of the collector is reached, additional heat transfer can be prevented. This prevents over-heating of the circulating fluid, which is a common problem in many applications of solar collectors. However, the heat pipe evacuated tubular solar collector must maintain a vacuum environment to sustain thermal performance. In practical applications, maintaining the vacuum environment is somewhat difficult, which is a disadvantage of heat pipe solar collectors. U-tube solar collectors are always connected with existing heating supply devices. The selective coating on the inner cover of the evacuated tube converts solar energy into heat energy and transfers heat to metal U-tubes through an aluminum fin. The liquid (usually a glycol-water antifreeze mixture) in the metal U-tube is heated. The U-tube then conducts the heat energy to the water inside the storage tank through a plate exchanger or internal spiral coils. The U-tube collector adopts the fins with a fast radiation speed, so it has the advantage of a high temperature and a fast heat transfer speed. Since there is no water in the vacuum tubes, the water scale will not come into being. There is no blast damage, so its lifetime is longer and its performance is better.

B. Previous studies

The applications of solar collectors have been studied extensively. There is a huge body of work that mathematically describes solar collectors. Some of them are basic books that contain the fundamentals of thermodynamic techniques, solar energy, or heat pipes. Dunn(1982) and Fadar(2009) studied a solar adsorptive cooling system using an activated carbon-ammonia pair in which the reactor was heated by a parabolic trough collector coupled with a water/stainless steel annular heat pipe. However, no experimental validation was provided. Beekley and Mather (1975) first developed a mathematical procedure to evaluate the collectible radiation on a single tube of evacuated heat pipe solar collectors, and Abdelrahman (1979) studied the direct absorption of concentrated solar radiation by the suspension of solid micro-particles in gas. Results show that the absorbed fraction of solar radiation is significantly dependent on the particle' s size and concentration in suspension. The effect of heat loss from the piping system of a large solar collector field was measured, and the effect of this loss on the effective collector efficiency was evaluated. It was found by Ali(2006) that the effect of piping loss on the effective collector efficiency was very similar: small in the mid-day and large in the morning and afternoon.

Ma et al. (2010) have made attempts to make clear theoretical analyses of heat loss coefficients and thermal efficiency for U-tube glass evacuated tube solar collectors that are influenced by the air gap between the copper fin and the absorber tube. They found that the influence is great. Tian(2006) studied thermal performance of the Dewar evacuated tube solar collector with an inserted U-pipe has been investigated in regard to energy balance. Yan(2008) showd unsteady

state efficiency of the Dewar tube solar collector with an inserted heat pipe has been studied. Additionally, a test of the thermal performance of the Dewar tube solar collector with air as the heat transfer fluid under dynamic conditions outdoors has been developed by Xu(2012). In addition, Han(2008) have expanded on the one-dimensional model and created a three-dimensional model.

In a recent study, He et al. (2011, 2012) designed the prototype of a solar thermoelectric co-generator (STECG) system that can supply either hot water or electric power, or both simultaneously, by incorporating TEGs into evacuated glass tube solar collectors. Hull (1986) investigated the heat transfer factors and thermal efficiency of a heat pipe absorber array connected to a common manifold and predicted an array with fewer than 10 heat pipes has significantly less efficiency than a conventional flow-through collector. Fernandez-Garcia (2010) presented a review of parabolic trough solar collectors and applications to supply high thermal energy.

C. Propose of this paper

Even though many studies have been carried out to improve thermal performance, but almost of paper shows in experimental result which leads to some difficulty to study theoretically and the cases without facilities, furthermore, it is difficult to find literature on the comparison of thermal performance characteristics for evacuated tube solar collectors with heat pipes and U-tubes. In this study, a theoretical model was developed to investigate thermal performance under variable operating conditions. It was then verified experimentally. In addition, thermal performance under each condition was compared with operating conditions

and analyzed.

I. Experiment setup

A. Experiment facilities and method

The solar collector of this study is a concentric evacuated tube collector that can be reliably operated to obtain heat for residential applications. For the working fluid, a water-propylene glycol mixture is used (with the ratio of water to propylene glycol being 80:20). The solar collectors are all south-facing with a tilt angle of about 45°, and the collector is located in Gwangju, Korea, where the latitude and longitude are 35° and 126°, respectively. The solar radiation collected per unit of absorber is different with the different tilt angles of the solar collectors, which leads to differences in the outlet temperature of the working fluid and in the efficiency of the solar collectors.

The closed-loop configuration of the test setup is shown in Fig. 2.1 The specifications of the test setup of the heat pipe and the U-tube type solar collector are also the same as the simulation study, which is shown in Table 2.1 The setup consists of ESCU, ESCHP, constant-temperature bath, heater, pump, and measurement facilities. The measurement devices include a pyranometer, flowmeter, and thermocouples. The physical quantities of working fluid temperatures at the inlet and outlet of the collector, the ambient temperature, the flow rate of the circulating water, and the incident solar irradiance were measured. The solar radiation was measured using a pyranometer that was installed on the solar collector. The aperture was leveled with the aperture of the collector without casting a shadow on the collector. The radiation was continuously recorded along with the rest of the data streams. Additionally, a

pyranometer was used to measure the incident beam radiation. The ambient temperature sensor was located behind the collector and away from direct irradiance. The temperatures were measured with thermocouples in the inlets and outlets of each component. A flowmeter was used to measure the flow rate of the circulating fluid, which was circulated by a pump. The water passed through the circulating pump and to both of the collectors, and then gathered in the constant-temperature bath to exchange heat with the water inside the tank and the flow into the flow meter and the water heater. The water flow rate was kept almost constant, around 0.065 kg/s.

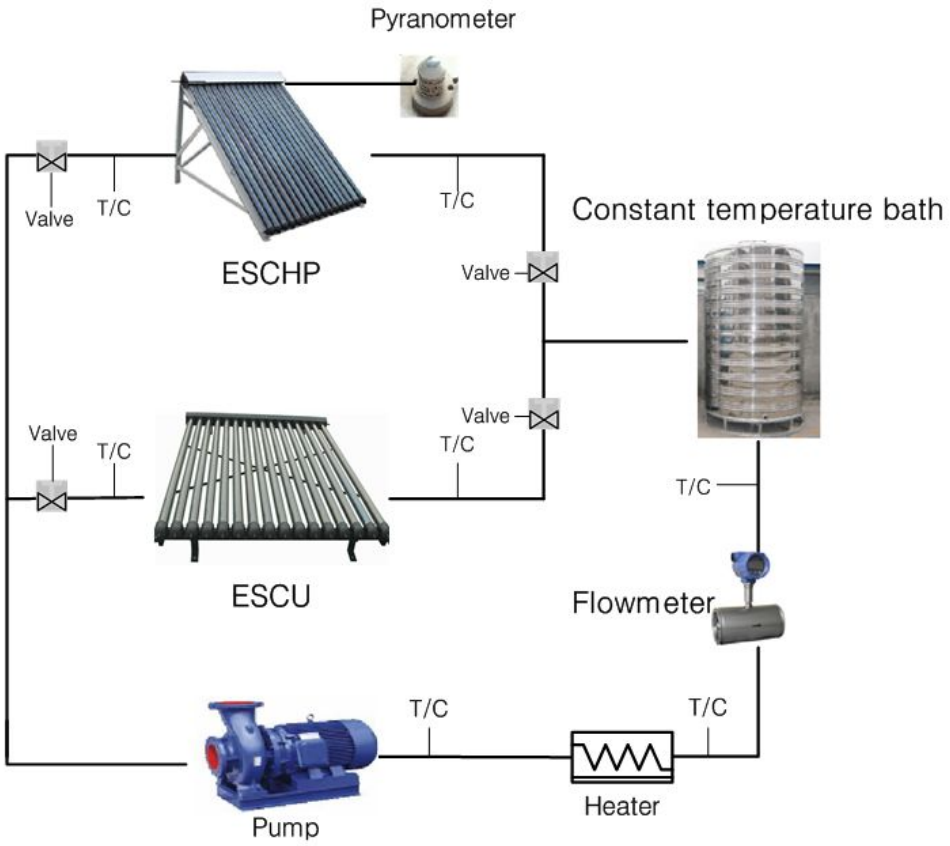

Fig. 2.1 Schematic diagram of solar collector test facility

Table 2.1 Specifications of solar collectors

ESCHP	ESCU
Outer tube out diameter = 47 mm Outer tube thickness = 2 mm Outer tube transmittance = 0.907 Outer tube reflectance = 7.5% Outer tube absorbance = 1.8% Absorptivity of the absorber part = 0.92 Emissivity of the absorber part = 0.08	
Heat pipe outer diameter = 8 mm Thickness of the heat pipe = 1 mm Heat pipe conductivity = 43 W/(mK) Condensing part length = 75 mm Condenser outer diameter = 14 mm Evaporating part length = 1670 mm Condenser inner diameter = 12 mm Absorber area = 2 m^2	U-tube outer diameter = 8 mm U-tube thickness = 1 mm Bond conductance = 30 W/(mK) Absorber tube thickness = 2mm Absorber area = 2 m^2 Copper fin thickness = 0.6 mm Copper fin conductivity = 307W/(mK) Absorber outer diameter = 37 mm Air gap= 1 mm Air gap conductivity = 0.03 W/(mK)

B. Measurement equipment

1. Thermocouple

A thermocouple is a temperature-measuring device consisting of two dissimilar conductors that contact each other at one or more spots. It produces a voltage when the temperature of one of the spots differs from the reference temperature at other parts of the circuit. Thermocouples are a widely used type of temperature sensor for measurement and control, and can also convert a temperature gradient into electricity. Commercial thermocouples are inexpensive, interchangeable, are supplied with standard connectors, and can measure a wide range of temperatures. In contrast to most other methods of temperature measurement, thermocouples are self powered and require no external form of excitation. The main limitation with thermocouples is accuracy; system errors of less than one degree Celsius (° C) can be difficult to achieve.

In this study, K-type thermal couple is used in the experiment, and which is shown in the Fig. 2.2, it used to test the inlet temperature, outlet temperature and ambient temperature.

As shown in the Table 2.2, it can test from -200°C to 300°C. Ansi standard limits of error is about 0.75% while Ansi special limits of error is just 0.4%

Fig. 2.2 Photograph of thermocouple K-type

Table 2.2 Specification of thermocouple

Item	Specification
Type	K-type
Range	-200 to 300℃
Ansi standard limits of error	0.75%
Ansi special limits of error	0.40%

2. Pyranometer

A pyranometer is a type of actinometer used to measure broadband solar irradiance on a planar surface and is a sensor that is designed to measure the solar radiation flux density (in watts per metre square) from a field of view of 180 degrees and is shown in the Fig. 2.3. The name pyranometer stems from Greek, A typical pyranometer does not require any power to operate.

In this study, it is used to measure the solar radiation to help the experimental study, the range of pyranometer is from 0~2000 W/m^2 and accuracy is about 0.15%.

To make a measurement of irradiance, it is required by definition that the response to "beam" radiation varies with the cosine of the angle of incidence, so that there will be a full response when the solar radiation hits the sensor perpendicularly (normal to the surface, sun at zenith, 0 degrees angle of incidence), zero response when the sun is at the horizon (90 degrees angle of incidence, 90 degrees zenith angle), and 0.5 at 60 degrees angle of incidence. It follows that a pyranometer should have a so-called "directional response" or "cosine response" that is close to the ideal cosine characteristic.

Fig. 2.3 Photograph of pyranometer

Table 2.3 Specification of thermocouple

Item	Specification
Type	Silicon pyranometer
Sensitivity	76
Range	0~2000(W/m^2)
Accuracy	0.15%

3. Flow meter

Flow measurement is the quantification of bulk fluid movement and is shown in the Fig. 2.4. Flow can be measured in a variety of ways. Positive-displacement flow meters accumulate a fixed volume of fluid and then count the number of times the volume is filled to measure flow. Other flow measurement methods rely on forces produced by the flowing stream as it overcomes a known constriction, to indirectly calculate flow. Flow may be measured by measuring the velocity of fluid over a known area.

Both gas and liquid flow can be measured in volumetric or mass flow rates, such as liters per second or kilograms per second. These measurements are related by the material's density. The density of a liquid is almost independent of conditions. This is not the case for gasses, the densities of which depend greatly upon pressure, temperature and to a lesser extent, composition.

When gases or liquids are transferred for their energy content, as in the sale of natural gas, the flow rate may also be expressed in terms of energy flow, such as GJ/hour or BTU/day. The energy flow rate is the volumetric flow rate multiplied by the energy content per unit volume or mass flow rate multiplied by the energy content per unit mass. Energy flow rate is usually derived from mass or volumetric flow rate by the use of a flow computer.

In this study, the flowmeter is used for measure the flow rate of the working fluid in the solar collector system and for the specifications is shown in the table 4.2.

Fig. 2.4 Photograph of flowmeter

Table 2.4 Specification of flow meter

Item	Specification
Output	4-20 mADC
Max Flow	1.4 m^3/hr
Power	100-240 VAC
Model	E-MAG-I
Size	1C A
Ser No.	191525

C. Experimental conditions

The experimental conditions are listed in Table 2.5. A cloudy day and a fair day were chosen for experimental verification to compare and investigate the thermal performance between the simulation and experimental results. The temperature on a cloudy day ranged from 1.5°C to 3.3°C, and the solar radiation ranged from 0 to 550W/m^2, while for the fair day, the temperature ranged from 4°C to 12.3°C, and the maximum solar radiation reached 1,150 W/m^2. All the measuring instruments were calibrated and run for a long time before starting the measurements to ensure the starting operation conditions of each type of solar collector were the same.

Table 2.5 Experimental conditions

Date	Mar 11th	Jan 5th
Weather condition	Fair day	Cloudy day
Mass flow rate of fluid	0.065 kg/s	0.065 kg/s
Total solar radiation	17.8 MW	6.7 MW
Average ambient temperature	10.6°C	2.3°C

II. Modeling of solar collector

A. Modelling of heat pipe type solar collector

1. Thermal analysis of heat pipe solar collector

In an evacuated heat pipe collector, a sealed copper pipe containing a vaporizable fluid was bonded to an absorber located inside the glass tube, as shown in Fig. 3.1. A copper condenser was attached on one side to the manifold part. The heat pipe in the collector consisted of an evaporating part and a condensing part. As the sun shone on the absorber, the pipe was heated and the liquid inside the pipe evaporated and rose toward the condenser part, after which it was cooled by the working fluid in the manifold. Then, the liquid returned to the bottom of the heat pipe. The vacuum tube minimized the heat loss of the collector. It increased the thermal performance and transferred a great deal of heat from the evaporator to the condenser.

As the working fluid flowed through the manifold, the heat was transferred from the condenser to the working fluid, the fluid was heated, and the temperature increased.

The following assumptions were made regarding the model: First is the temperature gradient in the longitudinal direction of the collector can be neglected cause of the change is small. Secondly, the working fluid in the manifold can absorb 100% of the heat transferred from the condenser. Thirdly, the overall heat loss coefficient between the collector and the surroundings is assumed to be constant.

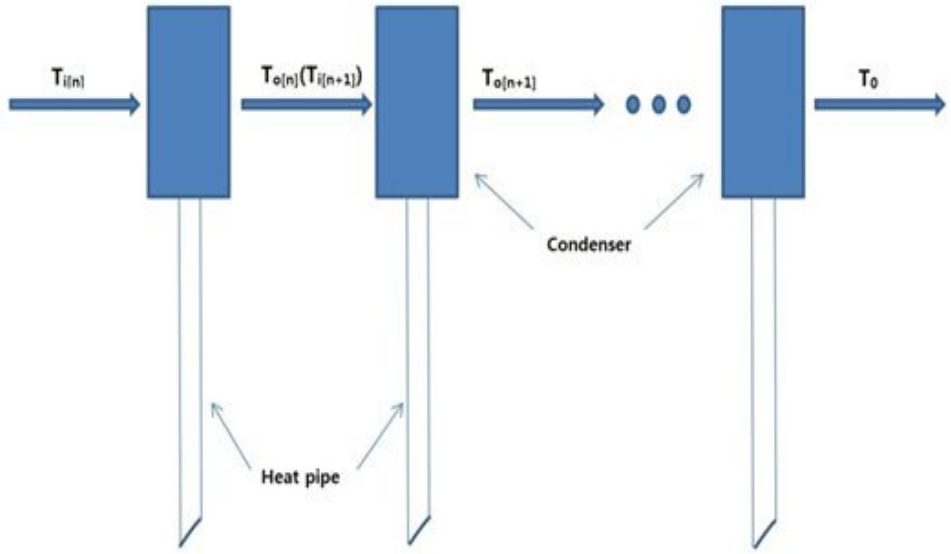

Fig. 3.1 System configuration of heat pipe type solar collector

One collector had 20 tubes, and for each one the thermal analysis method was the same, as shown in Fig. 3.1. Heat was transferred from the condenser to the working fluid flowing in the manifold, and as a result, the temperature of the working liquid in the first heat pipe reached T_o, which was also the inlet temperature for tube 2. The heat pipe solar collector was made up of many heat pipes, and the condenser of the heat pipes was mounted into a heat exchanger (manifold). The manifold was a copper pipe wrapped around each heat pipe condenser. The working fluid flowed through the manifold and picked up heat from the heat pipe condenser.

Fig. 3.2 showed the construction of a single heat pipe, as well as the heat flow. The following thermal analysis of the heat pipe solar collector is for a single pipe. The heat transferred from the evaporator to the condenser section in the

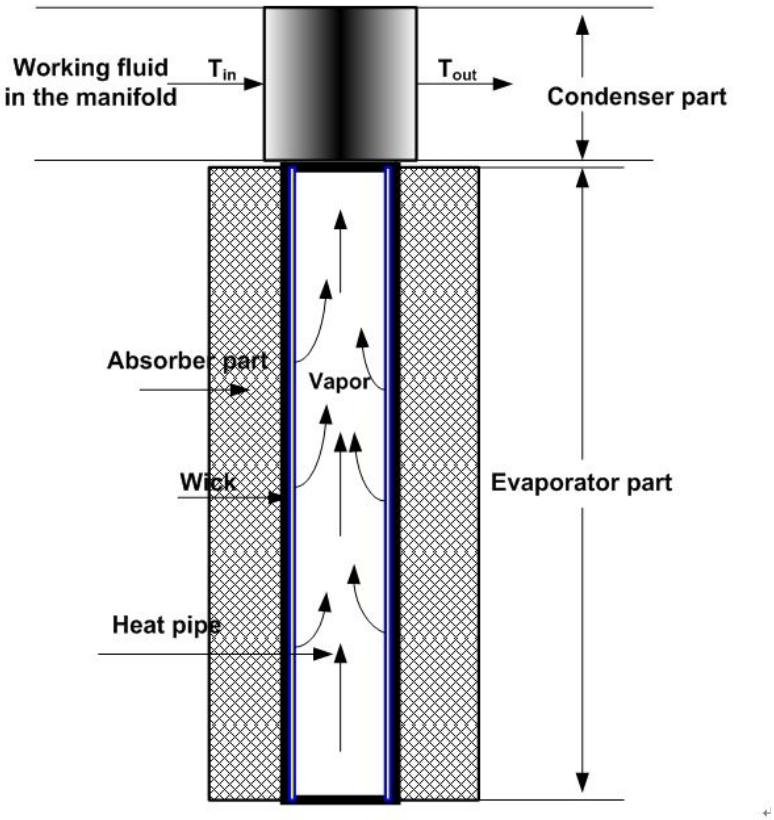

Fig. 3.2 Cross-section of single heat pipe and heat flow

heat pipe can be written as:

$$Q_{hp} = \frac{A_{hp}(T_{evap} - T_{con})}{\sum R_{hp}} \tag{3-1}$$

Where T_{hp} and T_{con} are the outer surface temperatures of the evaporator and condenser, respectively, and R_{hp} is the total thermal resistance of the heat pipe. In the vapor space, only the end-to-end temperature variations, which are caused

by vapor-flow pressure drops, are associated with changes in this section. The pressure drop is very small in the heat pipe, and the pressure in the vapor space is assumed to be at a constant saturation pressure. Since heat is absorbed by the heat pipe and in steady-state operation, the total heat absorbed by the heat pipe should be rejected at the condenser section. In the evaporator section, the thermal resistances that account for temperature drops are the wall and wick conduction resistances, and the internal thermal resistance at the evaporator can be represented using the film coefficient h_{evap}.

The heat transferred from a heat pipe to the working fluid in the manifold can be expressed as:

$$Q_{con} = U_{con} A_{con} (T_{con} - T_i) \tag{3-2}$$

Combining equations (3-1) and (3-2), the temperature of the outer surface of the condenser part can be derived as:

$$T_{con} = T_i + \frac{T_{evap} A_{hp}}{U_{con} A_{con} \sum R_{hp}} \tag{3-3}$$

The overall heat transfer coefficient of the condenser can be expressed as:

$$U_{con} = \frac{1}{\frac{t_{hp}}{k_{hp}} + \frac{1}{h_{con}}} \tag{3-4}$$

Where t_{hp} and k_{hp} are the thickness and conductivity of the heat pipe, respectively, and the heat transfer coefficient, h_{con}, can be derived from Azad(2008) :

$$h_{con} = \frac{Nuk}{D_{hy}} \tag{3-5}$$

The hydraulic diameter D_{hy} is equal to D_i-D_o, where D_i is the inner diameter of the flow channel and D_o is the outer diameter of the heat pipe. The cooling liquid flow in the manifold is a fully developed laminar flow, which has a Reynolds number less than 2,300 due to its very low velocity and relatively large cross-sectional area. It is assumed that the flow inside the condenser of the heat pipes is thermally developed and therefore under a constant heat flux boundary condition at the wall, the Nusselt number is constant and may be written as 4.364.

The thermal resistance of the heat pipe is the sum of the individual resistances. These resistances can be obtained from the equations given by Dunn and Reay(1982) , which are expressed as follows:

$$R_{hp} = \sum (R_{evap,p} + R_{evap,w} + R_v + R_{lv} + R_{con,p} + R_{con,i}) \tag{3-6}$$

Where, it includes the resistance across the thickness of the pipe, the wick of the evaporator, the liquid and vapor interface' s resistance, the resistance associated with the conduction process through the pipe wall of the condenser,

and the convective heat resistance of the evaporator and condenser.

$$R_{evap,p} = \frac{\ln(\frac{r_{o,p}}{r_{i,p}})}{k_p 2\pi L_{evap}} \tag{3-7}$$

$$R_{evap,w} = \frac{\ln(\frac{r_{o,w}}{r_{i,w}})}{k_w 2\pi L_{evap}} \tag{3-8}$$

$$R_{evap,lv} = \frac{2}{h_{evap}\pi D_{i,p} L_{evap}} \tag{3-9}$$

$$R_{con,p} = \frac{\ln(\frac{r_{o,p}}{r_{i,p}})}{k_p 2\pi L_{con}} \tag{3-10}$$

$$R_{evap,i} = \frac{1}{h_{evap}\pi D_{i,p} L_{evap}} \tag{3-11}$$

$$R_{con,i} = \frac{1}{h_{con}\pi D_{i,con} L_{con}} \tag{3-12}$$

2. Single-pipe thermal analysis

The useful energy gained by a single pipe and the rate of useful energy collected may be referenced following Hottel(1955), which can be written for this case as:

$$Q_u = A_c F_a [G(\tau\alpha)_e - U_L(T_{hp} - T_a)] \tag{3-13}$$

Where, T_a is the ambient temperature, F_a is the effective factor of the collector, is the effective transmittance-absorbance product, and is the solar collector heat transfer loss coefficient. The useful energy transferred in the form of heat by the fluid flowing in the manifold can be written as:

$$Q_u = C_p \dot{m}(T_o - T_i) \tag{3-14}$$

Combining equations (3-13) and (3-14), the temperature T_{hp} can be easily obtained, as follows:

$$T_{hp} = T_a + \frac{G(\tau\alpha)}{U} - \frac{T_o - T_i}{NTU_{hp}} \tag{3-15}$$

In the condenser part of the heat pipe, cold fluid cross-flows with the vapor flow in the heat pipe. For this special case, the heat exchanger behavior is independent of the flow arrangement. The effectiveness-NTU equation for this can be expressed as:

$$\epsilon_n = 1 - e^{-(NTU)_{con}} \tag{3-16}$$

$$\epsilon_n = \frac{T_o - T_i}{T_{con} - T_i} \tag{3-17}$$

For a collector with n pipes, the water flows in the manifold and through the heat pipe condensers to the second heat pipe, as shown in Fig. 3-1. The inlet temperature of second heat pipe is the first heat pipe' s outlet temperature. Thus, substituting equation (3-16) into (3-17), and combining with equation (3-3), the collector outlet temperature for a collector at n pipes can be written as:

$$T_o = T_i + \frac{\epsilon(T_{hp} - T_i)A_{hp}}{U_{con}A_{con}R_{hp}}(1 + \frac{A_{hp}}{U_{con}A_{con}R_{hp}}) \qquad (3\text{-}18)$$

B. Modeling of U-tube type solar collector

1. Thermal analysis of U-tube solar collector

To compare thermal performance with heat pipe-type solar collectors, the thermal performance of the individual glass evacuated U-tube-type solar collector was numerically investigated. The U-tube-type solar collector of this study consisted of a two-layered glass evacuated tube and an absorber tube. Air was withdrawn from the space between the two glass tubes, forming a vacuum. The solar energy could be absorbed by absorber coating. The diameters of the outer and inner glass tubes were assumed to be 47 mm and 37 mm, respectively. The absorber tubes of the solar collectors with a U-tube welded inside a circular fin were investigated. The illustration of all the glass evacuated U-tubes is given in Fig. 3.3(a), and a cross-section of the U-tube was shown in Fig. 3.3(b). The solar

energy of amount G absorbed by the selective absorbing coating was solar radiation reduced by optical losses, as shown in Fig. 3(a). The useful heat gain, which was equal to the solar energy transferred to the working fluid, was assumed to be equal to the difference between G and the thermal loss through the glass tube due to radiation, conduction, and convection. A one-dimensional analytical investigation for a single unit of the glass evacuated U-tube type solar collector was carried out for the analysis of thermal performance of the U-tube type solar collector. To simplify calculations without significantly losing accuracy, several assumptions were adopted:

- The loss coefficient from the header tube is also constant.
- The heat transfer process considered in the model is assumed to be steady, and transient phenomena are not included.
- The loss coefficient from the header tube is also constant.
- The air convection in the evacuated tube is neglected.

According to the energy balance law, the useful energy gained from the solar collector is equal to the solar radiation that the collector gathered to reduce energy loss to the environment, which is expressed as follows:

$$Q_u = I - Q_L \tag{3-19}$$

Where I is solar energy amount absorbed by the selective absorbing coating, and Q_u is the net heat gain absorbed by the working fluid. The overall loss coefficient can be defined as

$$U_L = U_t + U_{edge} \tag{3-20}$$

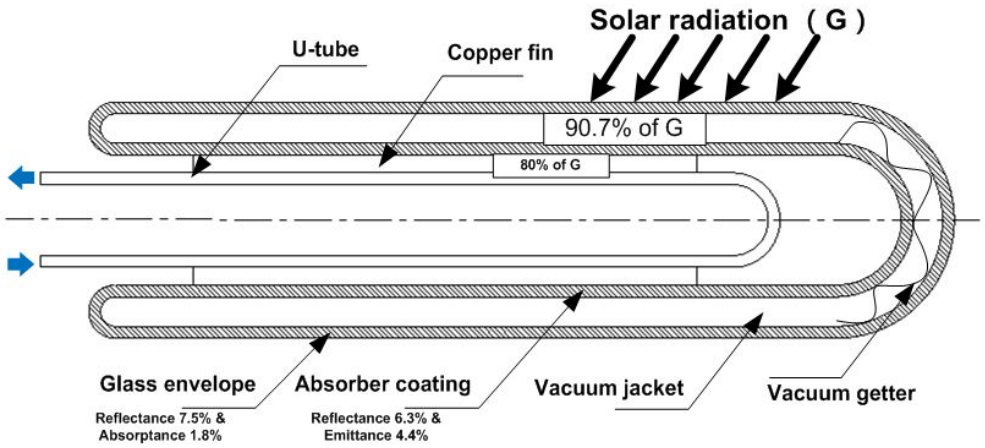

(a) Optical loss of glass evacuated tube

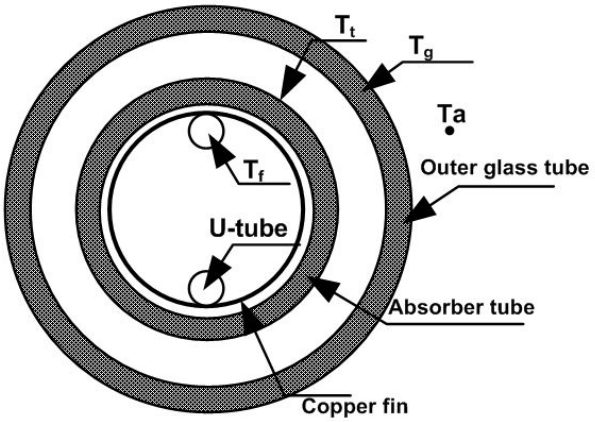

(b) Cross section of U-tube

Fig. 3.3 Illustration of evacuated U-tube

Where, U_{edge} is the edge loss coefficient of the header tube, which is 0.1687 W/(m^2K), and the loss coefficient from the absorber tube to the ambient U_t can be written as

$$U_t = \frac{1}{\frac{1}{h_{ga}} + \frac{1}{h_{pg}}} \tag{3-21}$$

Where h_{ga} is the convection heat transfer coefficient from the outer glass tube to the surrounding environment and referenced from Tian(2006). It is given about 12.7 W/(m^2K),and h_{pg} is the sum of h_{pgd} and h_{pgc}, which represents of heat transfer coefficient through conductivity and the radiation heat transfer coefficient between the absorber tube and the glass tube. According to Tian(2006), the outer surface area of the absorber tube, h_{pgc}, can be assumed by 0.2796 W/(m^2K).

$$h_{pgd} = \frac{\sigma \epsilon_c}{1 + \frac{\epsilon_c d}{\epsilon_g d_g (1 - \epsilon_c)}} (T_t^2 + T_g^2)(T_t + T_g) \tag{3-22}$$

Where ε_c is the emissivity of the absorbing coating, ε_g is the emissivity of the inner surface of the outer glass tube, d_g is the diameter of the glass tube, and σ is the Stefan-Bolzmann constant. In addition, the heat flux balance of the tube from Fig. 3 can be expressed as follows:

$$U_t (T_t - T_a) = h_{pgd} (T_t - T_g) + h_{pgc} (T_t - T_g) \tag{3-23}$$

From equations (3-21)~(3-23), the unknown parameters are T_t, T_a, U_t, h_{pgc}, and T_g. If the ambient temperature and absorber temperature are given, then U_t, h_{pgc}, and T_g can be decided with these equations.

To simplify the analysis, simple assumptions are also proposed. First, the absorber tube is parallel to the copper fin, so it can be regarded as the flat plate. This is because the absorber coating is very thin, so the temperature gradient in the radial direction is negligible, as is the temperature gradient in the flow direction along the tube. In Fig. 3.4, taking the width of Δx on an elemental region and unit length in the flow direction, the heat balance equation can be expressed as

$$-k\delta\frac{dT}{dx}|_x-(-k\delta\frac{dT}{dx}|_{x+\triangle x})+Q_u\triangle x=0 \tag{3-24}$$

$$Q_u=\frac{T_t-T}{\frac{t_c}{k_c}+\frac{t_{air}}{k_{air}}}=C_s(T_t-T) \tag{3-25}$$

Where t_c and t_{air} are the thickness of the absorber tube and the air gap, while k_c and k_{air} are the conductivity of the absorber tube and the air gap, respectively. C_s is the synthetic conductance.

Combined equations (3-19)~(3-21) can derive the expression of the absorber tube's temperature.

$$T_t=\frac{I+U_LT_a+C_ST}{U_L+C_S} \tag{3-26}$$

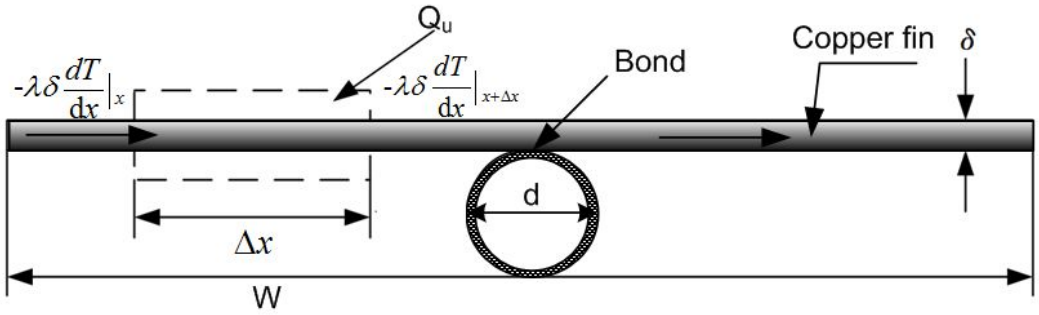

Fig. 3.4 Energy analyses on copper fin of ESCU

Substituting equations (3-25) and (3-26) into equation (3-20) can derive the energy balance equation as follows, while to solve the second-order differential equation, the boundary condition is needed.

The temperature's distribution expression can be calculated as follows, where in order to simplify the calculation.

$$T = \frac{\cos mx}{\cos(\frac{m(W-d)}{2})}(T_b - T_a - \frac{1}{U_L}) + T_a + U_L \tag{3-27}$$

The heat gain is equal to the sum of both sides of the energy collected from the U-tube and the energy collected above the tube region. At the same time, it is also equal to the energy transferred to the fluid. These two equations can be written as follows:

$$q_u' = \frac{(W-d)(I-U_L(T_b-T_a))F + d(I-U_L(T_b-T_a))}{1+\frac{U_L}{C_S}} \tag{3-28}$$

$$q_u' = \frac{(T_b - T_f))}{\frac{1}{h_{fu}\pi d} + \frac{1}{C_S}} \tag{3-29}$$

Where, h_{fu} is the heat transfer coefficient between the fluid and the U-tube wall. The fin efficiency of the straight fin F is given in the form

$$F = \frac{\tanh(\frac{m(W-d)}{2})}{\frac{m(W-d)}{2}} \tag{3-30}$$

Combining the equations to solve the t_b and substituting it into the equation (3-29), the net heat gain can be expressed as

$$q'_u = WF'(I - U_L(T_f - T_a)) \tag{3-31}$$

$$F' = \frac{\frac{1}{U_L}}{W(\frac{1+\frac{U_L}{C_S}}{U_L((W-d)F+d)} + \frac{1}{h_{fu}\pi d} + \frac{1}{C_b})} \tag{3-32}$$

Where F' is the collector efficiency factor and T_f is the average temperature of the working fluid in the U-tube.

The heat received by the fluid in the pipe is measured and given by

$$Q_u = \dot{m}C_p(T_o - T_i) \tag{3-33}$$

2. Modeling of the synthetical conductance

In this study, because of the influence of the air gap, four kinds of component are choose to investigate the improvement. As shown in the equation (3-25), Where δ_{ab} and δ_{com} is the thickness of the absorber tube and the filled component while the k_{ab} and k_{com} is the conductivity of the absorber tube and filled component, respectively. Considering the effect of filling problem, liquid is an ideal chose, as a result, water, benzene and Na-K alloy whose thermal conductivity are 0.62 W/(mK), 0.16 W/(mK) and 23 W/(mK) are choose as the component. C_b is the synthetic conductance which can be calculate as the denominator of the equation. Combined Eq. (3-19), (3-20) and (3-25) can derive the expression of the absorber tube' s temperature.

C. Thermal efficiency analysis of solar collector

The thermal efficiency of an evacuated solar collector with a U-tube and heat pipe is defined as the ratio between the net heat gain and the solar radiation energy based on the absorber area. The theoretical simulation equation for the thermal efficiency of a solar collector is:

$$\eta = \frac{\dot{m} C_p (T_o - T_i)}{AG} \tag{3-35}$$

Where m and C_p are the mass flow rate in manifold and specific heat of working fluid in the manifold, respectively.

The specifications of an evacuated solar collector with a U-tube and a heat pipe are shown in Table 3.1. To compare their thermal performance, total size, optical properties of outer glass tubes, and absorber areas, they must have the same specifications to minimize any mechanical influences on their performance.

Table 3.1 Properties of nanomaterial and base fluid

Material	Specific heat(J/kgK)	Thermal conductivity (W/mK)	Density(kg/m^3)
MWCNT	711	3000	2100
Water	4182	0.6178	992.2

D. Nanofluid properties calculation

k_{nf} is the conductivity of the nanofluid and comes from the conductivity of base fluid and nanopartical which referenced from Wu(2009).

$$k_{nf} = k_{bf}(1-\varphi) + \beta k_s \varphi \tag{3-36}$$

$$k_s = k_{bulk}\frac{0.75 d_s / l_s}{0.75 d_s / l_s + 1} \tag{3-37}$$

Where, k_{bf} and k_s is the conductivity of base fluid and nanoparticles, and k_{bulk}, d_s, l_s are the thermal conductivity of bulk material, characteristic length of nanoparticles and mean free path of heat carriers in nanoparticles, respectively.

Where, C_p is the specific heat of working fluid which can be calculated as follows,

$$(C_p)_{nf} = \frac{(1-\varphi)\rho_{bf}(C_p)_{bf} + \varphi\rho_s(C_p)_s}{\rho_{nf}} \tag{3-38}$$

$$\rho_{nf} = (1-\varphi)\rho_{bf} + \varphi\rho_s \tag{3-39}$$

$$\varphi = \frac{\frac{W_{nf}}{\rho_{nf}}}{\frac{W_{nf}}{\rho_{nf}} + \frac{W_{water}}{\rho_{water}}} \tag{3-40}$$

Where, ρ_s is the density of nanopartical which is 2100 kg/m^3, ϕ is the percentage of volume concentration, W_{water} = 100 g, W_{nf} is the weight of

nanocomposite and ρ_{water} = 998.5 kg/m^3. Considering the small size and the low volume fraction of the particles in most nanofluids, it might be reasonable to treat nanofluids as pure liquids in certain cases. Predicted values for single phase fluid from the existing Shah(1975) equation is as follows:

$$N_u = \begin{cases} 1.953(RePr\frac{d_i}{x})^{\frac{1}{3}} & (RePr\frac{d_i}{x} \geq 33.33) \\ 4.364 + 0.0722(RePr\frac{d_i}{x}) & (RePr\frac{d_i}{x} < 33.33) \end{cases} \tag{3-41}$$

$$h_{nf} = \frac{N_u k_{nf}}{d_i} \tag{3-42}$$

Where, x is the length of section considered and d_i is the inner diameter of the U-tube, the Reynolds number for flow in a circular tube is defined as Eq. (3-43) and viscosity can be calculated by the equation developed by Brinkman(1952).

$$Re = \frac{4\dot{m}}{\pi d \mu_{nf}} \tag{3-43}$$

$$\mu_{nf} = \frac{\mu_{water}}{(1-\varphi)^{2.5}} \tag{3-44}$$

III. Results and discussion

A. Analysis and verification of simulation results

1. Measured weather data on fair and cloudy day

Figs. 4.1 and 4.2 shows the experimental results of solar radiation and ambient temperature on two particular days. As shown in Fig. 4.1, the cloudy day had lower ambient temperature and poor solar radiation. Since thick clouds blocked the sunlight, the solar radiation was quite unsteady. This increased the difficulty for the pyranometer to collect data of the solar radiation, which was continuously recorded along with the rest of the data streams. The average radiation was nearly 266 W/m^2, and the ambient temperature measured behind the collector was about 2.3°C.

Fig. 4.2 shows the experimental result on a fair day, on which the radiation and the ambient temperature were relatively high, and the solar radiation was relatively steady. The average ambient temperature during operation was 10.6°C, and the average radiation was 617 W/m^2. As mentioned already, with high radiation and less difference between the ambient and inlet temperatures, the thermal performance of the solar collector is better, but unsteady factors such as clouds causing erroneous data in the process of the experiment are inevitable. Some prework such as deleting these bad points should be performed on the data.

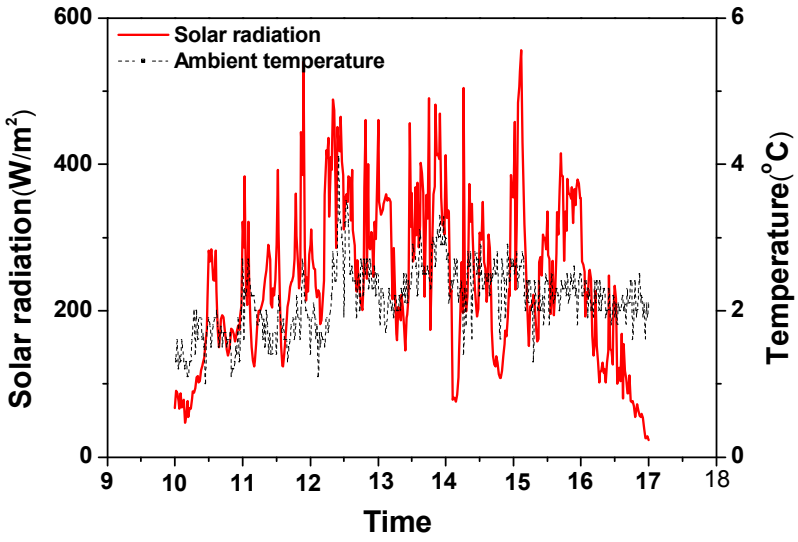

Fig. 4.1 Solar radiation and ambient temperature on cloudy day(Jan 5th)

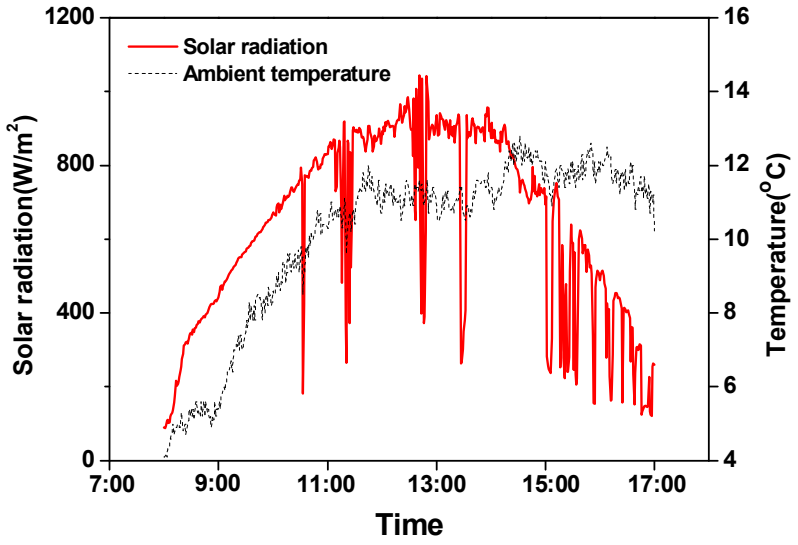

Fig. 4.2 Solar radiation and ambient temperature on cloudy day(Mar 11th)

2. Simulation results of solar collectors with various operating conditions

For simulation of efficiency of solar collector, according to the change of solar radiation and ambient temperature, is shown in Fig. 4.3 The inlet temperature of the solar collector is defined as 303 K, and the mass flow rate of the working fluid is set as 0.01 kg/s. Seen from Fig. 4.3, which is for the heat pipe solar collector, the efficiency will increase with solar radiation, and a higher ambient temperature will result in higher efficiency with the same collector inlet conditions. Under the given ambient temperature conditions, the efficiency of the collector increases sharply, to nearly 400~500 W/m^2, and the rate of increase decreases gradually and finally becomes almost steady. In addition, in this 3-D analysis chart, when solar radiation is smaller than 140 W/m^2 and corresponding ambient temperature is 270 K, the solar collector will not work properly due to the low absorbed energy.

The efficiency variation with solar radiation and ambient temperature of the U-tube-type is given in Fig. 4.4, which indicates the same tendency with the heat pipe-type: the higher solar radiation and ambient temperature will correspond to a higher efficiency, and the efficiency of the collector will increase sharply to nearly 200~300 W/m^2 and gradually come to a constant. From these two figures, it can be found that ESCU starts working earlier than ESCHP under low solar radiation conditions, and ESCHP's peak efficiency is higher than ESCU. Additionally, from the ambient temperature's perspective, the efficiency first increases gradually until the ambient temperature is equal to the inlet

temperature of the working fluid(303K). It will then keep falling.

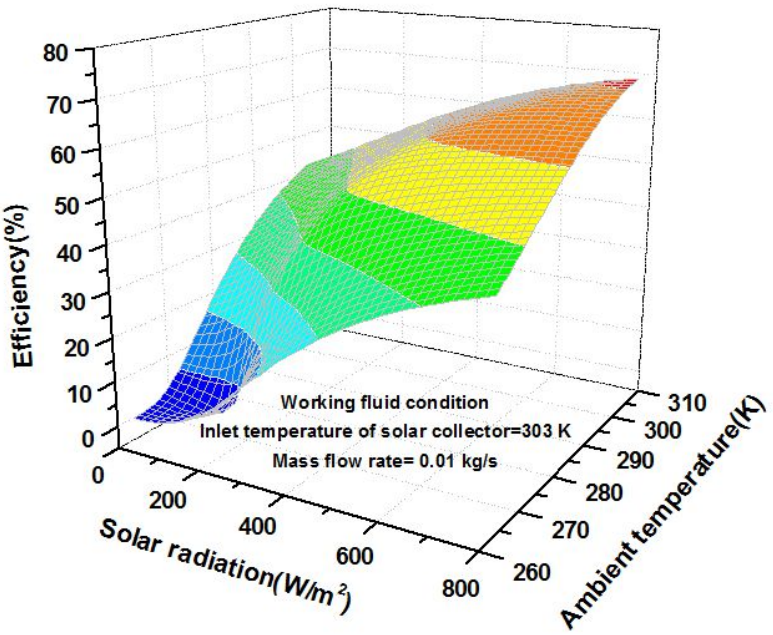

Fig. 4.3 Efficiency variation of ESCHP with T_a and G.

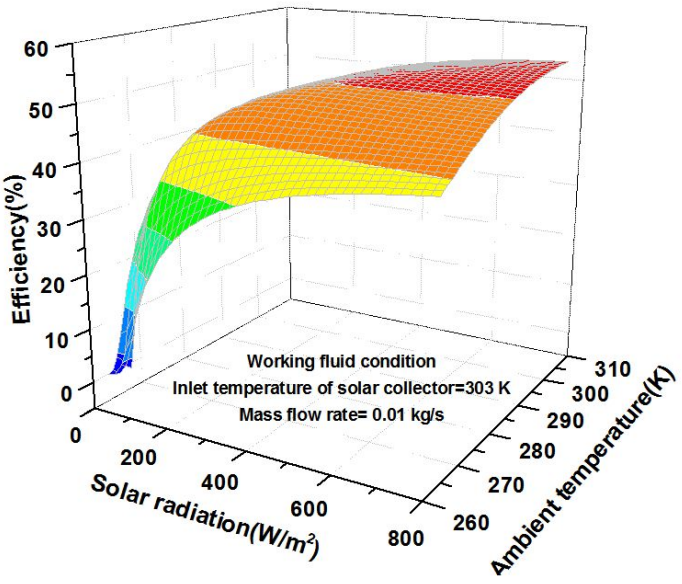

Fig. 4.4 Efficiency variation of ESCU with T_a and G.

3. Verification of two kinds of solar collector

To examine the reliability of the analytical method, the efficiency of the solar collector was compared to the experimental results. Fig. 4.5 shows the comparison of efficiency in two kinds of solar collectors; one is heat pipe solar collector which is shown in Fig. 4.5(a), and the other is U-tube solar collector which is shown in Fig. 4.5(b). The results show the accordance between the simulation and experimental ones, the deviation was not significant compared to the experimental results. In this study, the simulation and experimental results of the efficiency of solar collectors both showed the same trend: it decreased proportionally with the x axis, in which the temperature' s D-value directly influenced the useful energy collected by the solar collector. In addition, with the increase of solar radiation, the collector' s efficiency was also increased. The fitted correlation can be written as y = -274.68x + 74.1 and y = -208.3x + 58.25, while the R-square values are 0.99 and 0.98, respectively. The mean deviation for the ESCHP between the experimental and simulation results are about 3%, and the maximum error is about 5%. Mean deviation between simulation and experiment results are only 2%, while the maximum is about 4% for ESCU. These results indicate that the analysis method in this study was reasonable, and that it was accurate in analyzing the thermal performance of these two types of solar collectors. The small differences between the model and the experiment in the storage temperatures were a consequence of the fact that the pipes between the storage and the solar collectors were not insulated perfectly in the experiment.

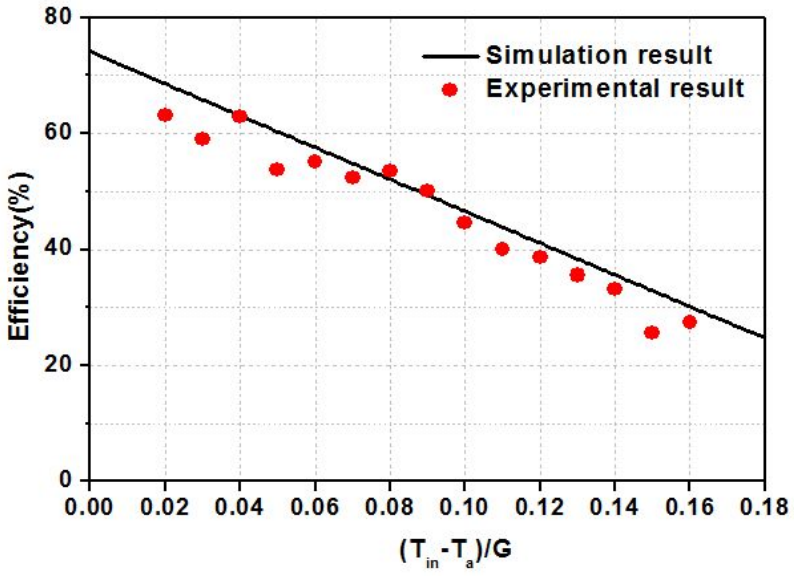

(a) Efficiency variation of the ESCHP

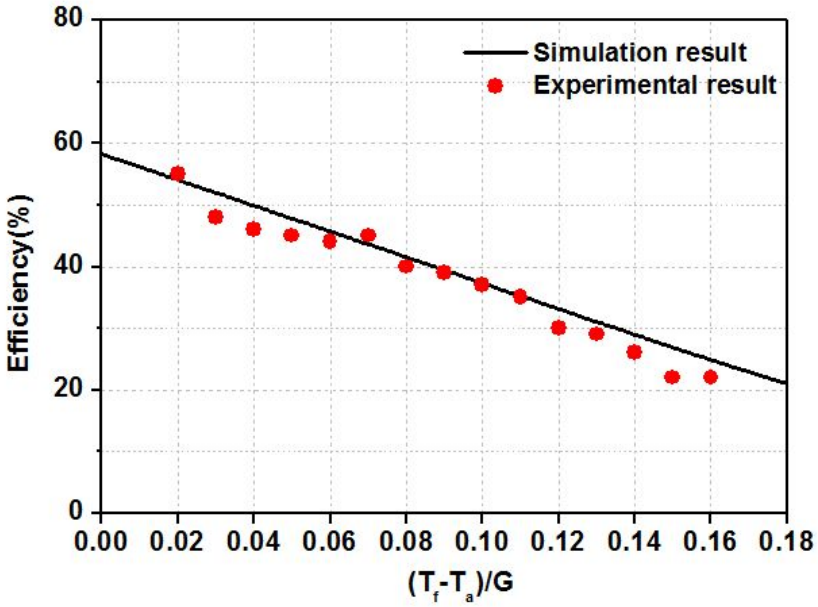

(b) Efficiency variation of the ESCU

Fig. 4.5 Comparison of efficiency in two types of solar collectors.

4. Efficiency with different conditions of $T_{in}-T_a$

Fig. 4.6 shows the relationship between the solar collector efficiency and the difference between the collector inlet temperature and the ambient temperature for both solar collectors. Generally, the difference between T_{in} and T_a is an important factor that affects the thermal performance of solar collectors. The value of $T_{in}-T_a$ ranges from 10 K to 35 K under different radiation conditions. This information indicates that a smaller difference between T_{in} and T_a corresponds to a higher efficiency.

As a result, for ESCHP, the greatest efficiency that appears with a temperature gap of 10 K is about 70%, while the efficiency decreases to 62% with a temperature gap of 35 K. As shown in Fig. 4.6, the gaps in efficiency between 200 and 800 W/m^2 were 10.6% and 35.1% for $T_{in}-T_a$ values of 10 K and 35 K, respectively. The same is the case for ESCU, where a lower difference of $T_{in}-T_a$ corresponds to a higher efficiency, and the gap between $T_{in}-T_a$ values of 10 K and 35 K is 2% and 7%, respectively.

Comparing the two types, it is easy to find the heat pipe-type one definitely has a higher efficiency in the solar radiation of 800 W/m^2, but it has a higher slope when the solar radiation is 200 W/m^2. Besides, when the $T_{in}-T_a$ is smaller than 17 K, the ESCHP performs better, while with the increase of difference of the T_{in} and T_a, it will be exceeded by the ECSU. In addition, the decrease in the collector's efficiency increases with the reduction of solar radiation. This helps to explain the phenomenon that under the same radiation conditions, the efficiency in the winter is lower than in the summer because the temperature difference of T_{in} and T_a is much larger. In the winter, the collected heat may

decrease, and it is difficult to maintain the hot water in the collector, which leads to a decrease in the thermal performance of the solar system.

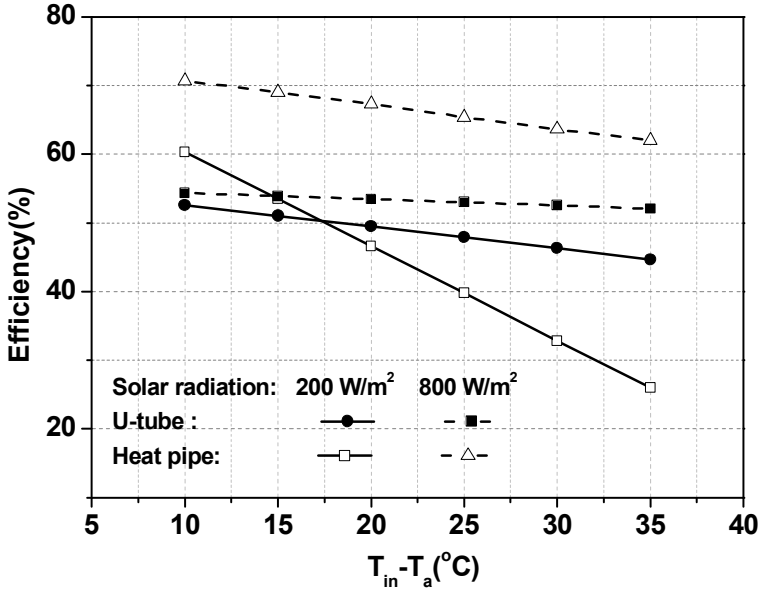

Fig. 4.6 Variation of solar collector efficiency with different conditions of T_{in}-T_a

B. Comparison of two kinds of solar collectors

1. Comparison under same operation condition

Fig. 4.7 gives a comparison of the two kinds of solar collectors on efficiency, and the operation condition is shown in the figure as the ambient temperature of 273 K, while the mass flow rate of the working fluid is 0.01 kg/s. In low solar radiation conditions, efficiency in both types increases rapidly, but the U-tube-type's increment is larger before solar radiation reaches nearly 450~550 W/m^2, ESCU's performance is better than ESCHP, and it is then exceeded by the heat pipe-type. When the radiation is less than 100 W/m^2, ESCU's efficiency increases rapidly, but ESCHP's efficiency maintains zero, which means that only ESCU is usable in this condition. Thus, it can be seen, under the fixed ambient temperature, that an evacuated solar collector with a U-tube is more efficient in low solar radiation conditions, and evacuated solar collectors with heat pipes fit high solar radiation conditions better. When the temperature of the inlet working fluid changes from 313 K to 323 K, it can be seen that the intersection of the two types moves to the right: 450, 500, and 540 W/m^2 for 313, 318, and 323 K, respectively. Furthermore, the efficiency gap of ESCHP between different inlet temperatures is larger than that of ESCU. It follows that with the increase of the difference between the inlet temperature of working fluid and ambient temperature, the efficiency intersection of the two types of solar collectors will move to a higher solar radiation.

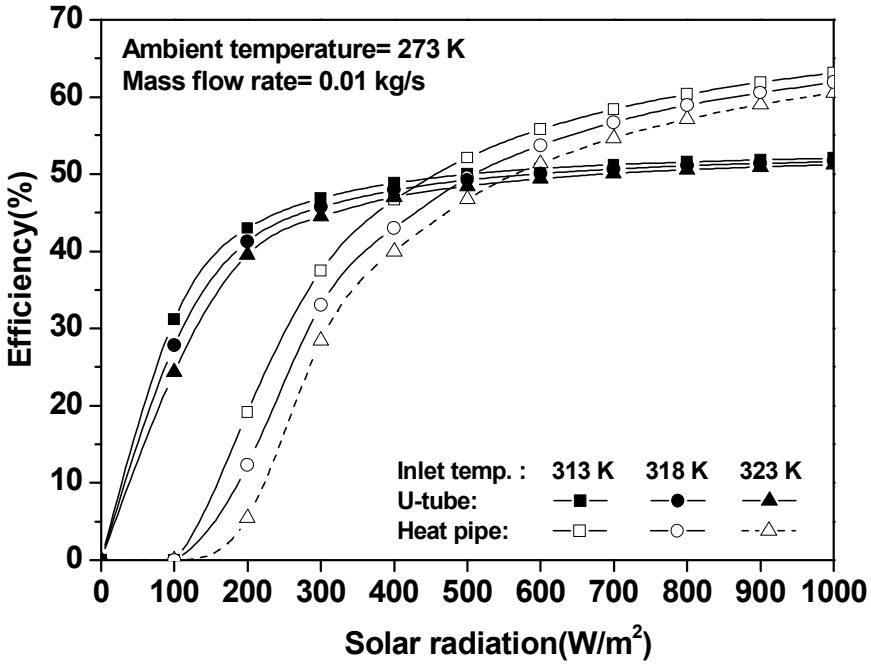

Fig. 4.7 Comparison of the efficiency of two kinds of solar collectors

2. Thermal performance of solar collectors on cloudy day and fair days

Figs. 4.8 and 4.9 show the experimental results of solar radiation and ambient temperature on two particular days. As shown in Fig. 4.8, the cloudy day has a low ambient temperature and poor solar radiation, and since thick clouds blocked the sun light, the solar radiation was quite unsteady. This made it more difficult for the pyranometer to collect data on the solar radiation, which was continuously recorded along with the rest of the data streams. The average radiation for cloudy was nearly 266 W/m^2, and the ambient temperature measured behind the collector was about 2.3°C.

Fig. 4.9 shows the experimental result on a fair day in which the radiation and ambient temperature were relatively high, and the solar radiation was relatively steady. The average ambient temperature during operation was 10.6°C, and the average radiation was 617 W/m^2. As mentioned, with high radiation and less difference between ambient and inlet temperatures, the thermal performance of the solar collector is better, but unsteady factors, such as clouds causing erroneous data in the process of the experiment, are inevitable.

In comparing the simulation results on a cloudy day, the heat pipe-type keeps a low and unsteady efficiency range from 5%~43%, while the U-tube shows better efficiency and remains at a stable efficiency that ranges from 40%~47% and higher than the heat pipe-type all the time, and an average deviation of around 17%. By contrast, on a fair day, due to the abundant solar radiation and ambient temperature, ESCHP's efficiency is around 50~60%, while for ESCU, it is just

50%, and ESCHP can only be exceeded after 4:30 in the afternoon. The mean difference between the two types is over 8% on a fair day. Thus, it can be seen that for the low radiation days, ESCU performs better than ESCHP and starts earlier, has more working hours, and keeps a steadier and relatively higher efficiency. On the contrary, for the fair days, ESCHP shows higher efficiency compared to ESCU.

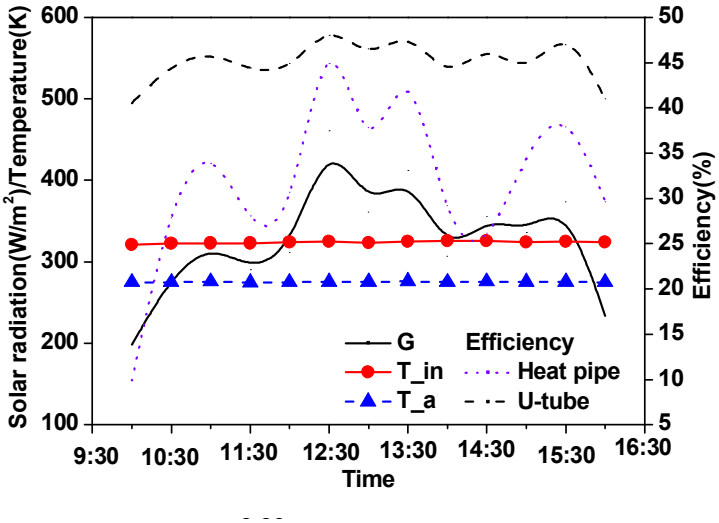

Fig. 4.8 Thermal performance of solar collector on cloudy day (Jan 5th)

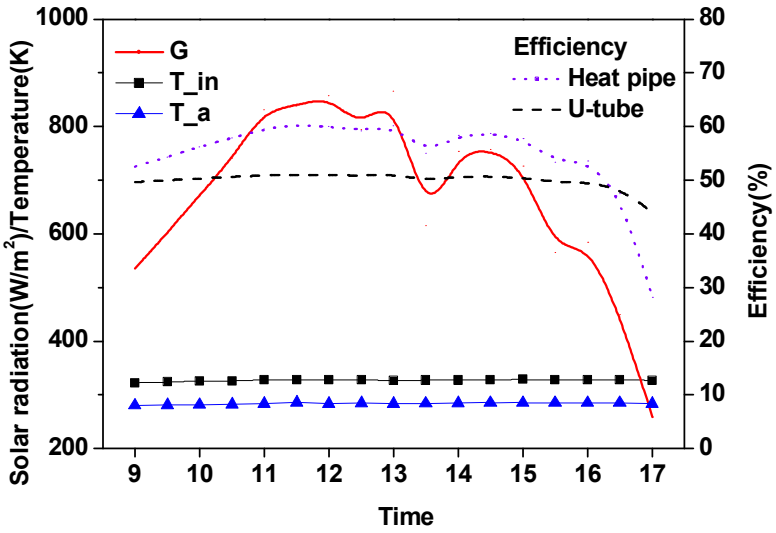

Fig. 4.9 Thermal performance of solar collector on fair day (Mar 11th)

C. Influence of synthetical conductance on the U-tube solar collector with MWCNT nanofluid

1. Variation of nanofluid properties on volume concentration

Fig. 4.10 shows the variation of specific heat, density and conductivity according to volume concentration of nanofluid. The density of nanofluid is proportional to volume concentration of nanoparticles, it can be explained by the Eq. (3-39), it increases from 992.2 kg/m^3 to 1003 kg/m^3 when the volume concentration increase to 1 vol%, the properties of MWCNT and water are shown in the Table 3, similarly, the conductivity of nanofluid is also proportional to the volume concentration of nanoparticles, which increased 15% when the volume concentration is 0.3 vol% and about 50% in 1 vol%. On the contrary, specific heat of nanofluid is inversely proportional to volume concentration of nanoparticle. Substitution of lower value of specific heat of nanoparticles from Table 3.1 will decrease the overall specific heat of nanofluid as shown in Eq. (3-38). Specific heat can be explained as the energy required raising the temperature of a unit mass of a substance by one degree. It means that a different amount of heat energy is needed to raise the temperature of similar masses of different substances by one degree. Smaller number of specific heat for nanofluid will leads to smaller amount of energy needed to raise the temperature.

Fig. 4.11 gives the variation of the heat transfer coefficient between working

fluid and tube with respect to Reynolds number for the nanofluids of various MWCNT volume concentrations. It is seen that the Nusselt number increases with increase of Reynolds number for a given MWCNT concentration. Compared to water, nanofluid applied with nanoparticle shows a significant enhancement on the Nusselt number, and Nusselt number is proportional to Reynolds number. In addition, it is seen 0.24% of volume concentration has higher heat transfer coefficient between fluid and U-tube wall than other cases of volume concentration under its steady state and it has averagely increased about 8% compared to water.

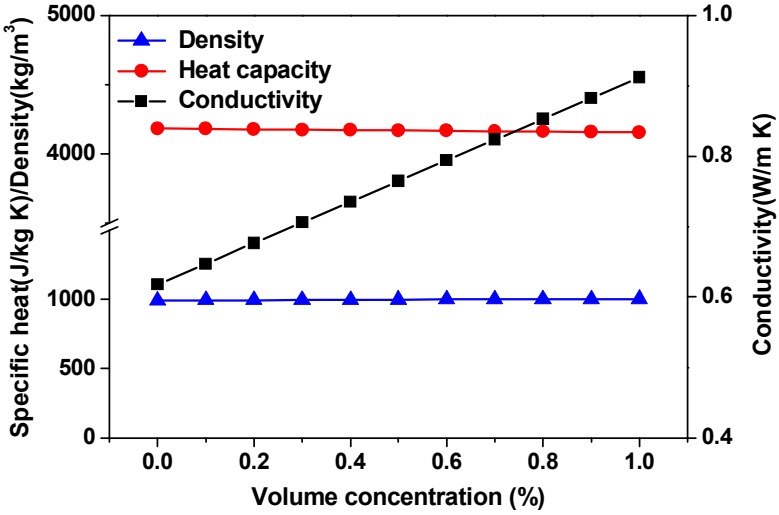

Fig. 4.10 Variation of nanofluid properties with volume concentration

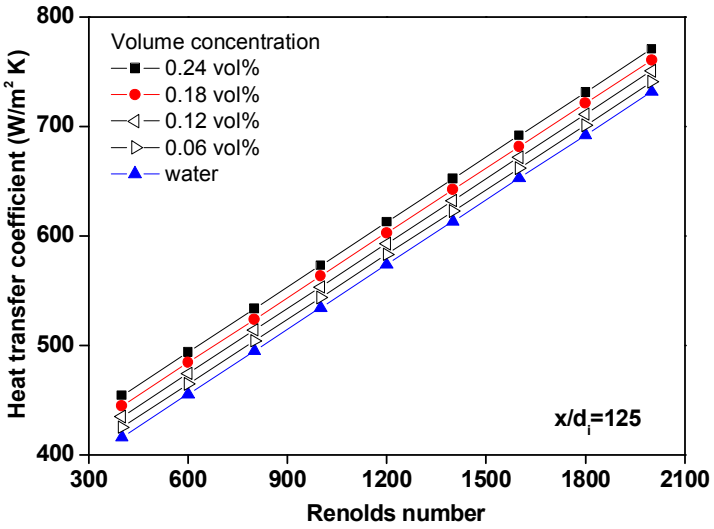

Fig. 4.11 Heat transfer coefficient versus Reynolds number

2. Synthetical conductance's effect on the thermal performance of solar collector

Heat transfer coefficient through conductivity between absorber tube and the glass tube will change by the difference of the temperature of the absorber tube and the ambient temperature, as shown in the Fig. 4.12, the radiation heat transfer coefficient increases with increase of temperature difference T_p - T_a. It' s nearly about 60% increment of H_{pgd} when T_p-T_a ranges from 0 ~ 70 K. It is not linear relation with ambient temperature and temperature difference T_p-T_a. In addition, the temperature increment of outer glass tube is also not linearly with difference between T_p and T_a. Furthermore, it is also incremental when the ambient temperature increases if the temperature difference T_p-T_a is given, which indicates the thermal loss will be increased with rise of the absorber tube temperature. Owing to the larger radiation heat transfer coefficient from absorber tube to the glass tube, the outer glass tube temperature increases, the difference is about 6 K when T_p-T_a ranges from 0 ~ 70 K.

Fig. 4.13 shows the variations of solar collector' s efficiency and absorber coating' s temperature with various synthetical conductance when solar radiation is set as 1000 W/m^2 and ambient temperature is 283 K, inlet temperature of working fluid of the solar collector is 313 K. It is found that from the result can see the influence of the synthetical conductance is significant and the efficiency ranges from 22% to 53% when C_b changes from 1 to 30 W/(mK), it also can be found that when C_b is larger than 80 W/(mK), the change can be neglected, in which case the change is within 0.1% per increment of 10 W/(mK), in other

words, the thermal resistance of air gap can be ignored in this case. According to the Eq. (3-25), define the thickness and conductivity of absorber tube is 1.2 mm and 1.2 W/(mK), and the thickness of the air gap is 1.5 mm, the critical point of component's conductivity is about 0.17 W/(mK). In addition, the influence of C_b on absorber coating's temperature is large.

Fig. 4.14 gives the variation of collector's efficiency with solar radiation. The efficiency will increase with the rise of solar radiation while the ambient temperature is fixed, and gradually comes to a constant. In this study 4 kinds of component between copper fin and absorber tube is studied. The results indicates higher conductivity will correspond to a higher efficiency, especially compared to the air gap one, the gap between Na-K alloy and air is about 2.3% in the 100 W/m^2 and 4% in the 900 W/m^2 which increases with the rise of the solar radiation. On the other hand, when the synthetical conductance of the component is bigger than 0.17 W/(mK), the change can be neglected, seen from the results that the difference between C_6H_6 and Na-K alloy is 0.3% in the 100 W/m^2 and increase to 0.6% in the solar radiation of 900 W/m^2 while for the differences between water and Na-K alloy are 0.1% and 0.2%. The results proved the conclusion of Fig. 4.13 that the efficiency will increase with the increase of conductance of the component between copper fin and absorber tube, but will gradually come to a constant, due to the similar results between benzene, water and Na-K alloy, taking other factors into consideration such as avoiding chemical reaction between them and copper fin, and the dangerousness of Na-K, thus water is a good choice because of its relatively higher conductivity compare to the critical conductance of 0.17 W/(mK) while the air gap is just 0.025 W/(mK). In addition, water will not increase the cost of the system significantly due to the

quantity needed is not big and it will not corrode the copper fin.

Fig. 4.15 gives the variation of solar collector's efficiency and absorber coating's temperature using different components with different mean temperature of working fluid. From Fig. 4.15 indicates that the efficiency of solar collector will decrease when the mean temperature of fluid in the u-tube increases, and Na-K shows the best performance in those components while the mean gap compared to air is about 3.6%, the difference between water and Na-K is just 0.1%. In the same way, it signifies absorber coating's temperature is proportional to the mean temperature of fluid in the U-tube, and the higher thermal conductivity of component is, the lower absorber coating temperature is. The mean deviation between Na-K and air is nearly 42 K while between water and Na-K is 3 K, and as said in the Fig. 4.12, higher absorber tube's temperature will lead to a higher thermal loss and decrease the efficiency of the solar collector.

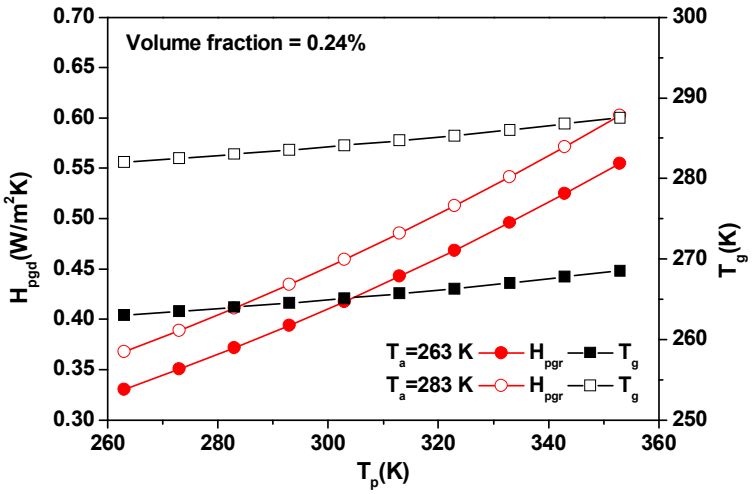

Fig. 4.12 Variation of H_{pgd} and T_g with the absorber coating temperature

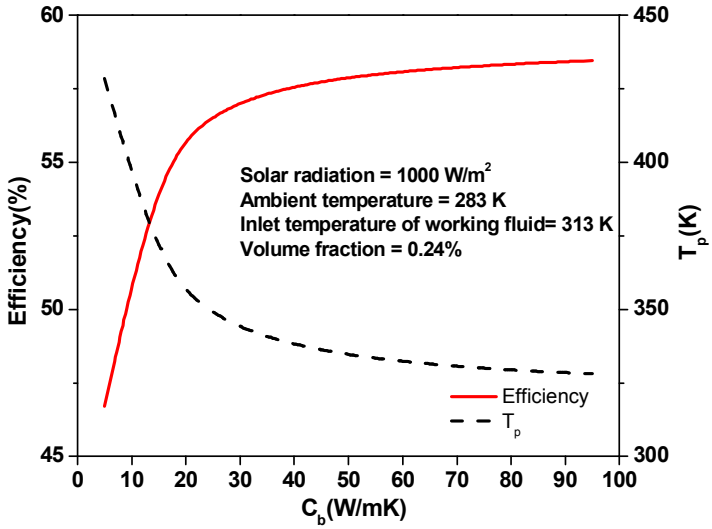

Fig. 4.13 Influence of synthetical conductance on the collector's efficiency and absorber coating temperature

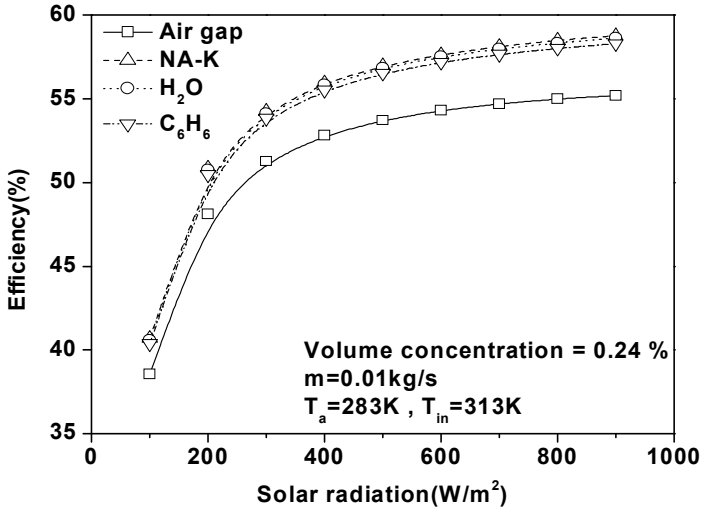

Fig. 4.14 Efficiency of solar collector using different components according to solar radiation

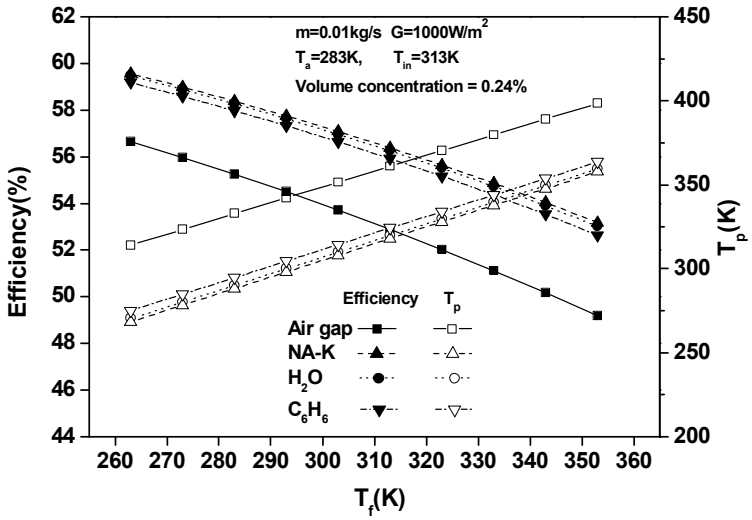

Fig. 4.15 Solar collector's efficiency and absorber coating's temperature using different components with different mean temperature of working fluid

3. Contributions on environment and economic

Fig. 4.16 shows the energy enhanced by applying water into the air gap. It can be seen that daily energy enhanced for one solar collector ranges from 785 kJ in July to 1200 kJ in October. When calculated into monthly energy enhancement, October shows highest which is 37.2 MJ per solar collector, while July has the lowest energy enhancement which about 25 MJ. Ordinarily for the solar collector arrays, the plenty of solar collectors have used, which indicates the influence for the improvement would be getting larger. In this study, it would be nearly about 18,008 MJ for one year by using 50 solar collectors.

Generally, coal equivalent is equal to 29306 kJ which means when 1 kg coal equivalent is completely combusted it can release 29306 kJ. But the same time it will release CO_2 and SO_2 to destroy the atmosphere and may intensify the greenhouse effect. After calculation, enhanced energy for solar collector in a year is equal to 12.3 kg of coal equivalent and will release 32.3 kg of CO_2 and 0.105 kg of SO_2, the variation of weight of coal equivalent and pollutions released on the number of solar collectors are shown in Fig. 4.16(a). It is seen that when the array has more than 50 solar collectors the amount of released pollutions are definitely huge and actually for an area like a city or even a state. It will release 1611.3 kg CO_2 and 5.228 kg SO_2 when the array has 50 solar collectors. When the plenty of solar collectors was installed, the amount of pollution saved can be very meaningful. In another way, as shown in Fig. 4.16(b), if consider the economical factor, when transfer the energy saved in a year to electricity power, it can be saved by 5002 kWh for 50 solar collectors which is from Lindsay. In addition, it can be calculated that the cost is more than 1750 dollars for Germany

for 50 solar collectors and about 1000, 600 and 400 dollars for UK, USA and China, respectively.

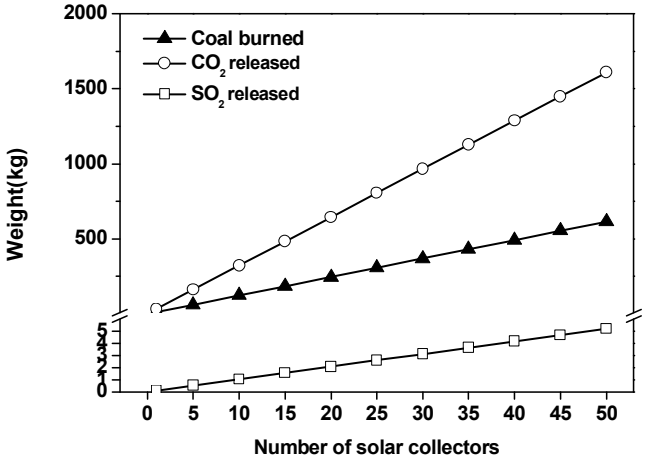

(a) Variation of weight of coal equivalent and pollutions released on the number of solar collectors

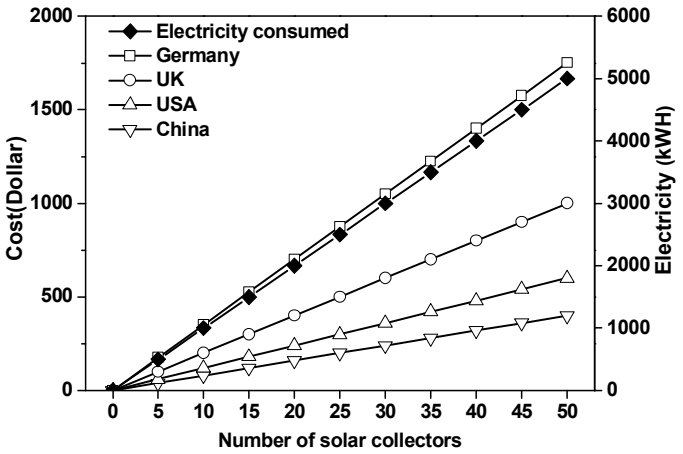

(b) Cost of electricity which equals to the saved energy in some countries

Fig. 4.16 Environmental and economic factor analysis

IV. Conclusion

Evacuated solar collectors with heat pipes and U-tubes were investigated both theoretically and experimentally, and a method of calculating the efficiency of the collector and the outlet temperatures using thermal analysis was introduced. The model predictions were validated using experimental data. The agreement between the measured and calculated storage temperatures was very good. It has been shown that collector efficiency will increase rapidly in low-radiation situations, while staying relatively steady with high radiation and small differences between the inlet temperature of a solar collector and ambient temperature will correspond to a higher efficiency.

Comparing the simulation results between ESCU and ESCHP, the U-tube-type became steadier and more efficient in the low solar radiation condition, while the heat pipe-type had better thermal performance in the high solar radiation condition. ESCHP can reach more than 60% when both the ambient temperature and solar radiation are sufficient, while ESCU keeps a steady output regardless of the condition. In addition, when the inlet temperature of the working fluid increases, the efficiency intersection of the two types of solar collectors will move to the higher solar radiation, which means that the solar radiation of ESCHP needs to exceed that of ESCU to become larger. For low radiation days, such as cloudy or rainy days, ESCU performs better than ESCHP and starts earlier, has more working hours, and keeps a steadier and relatively higher efficiency; on the contrary, on fair days, ESCHP shows a higher efficiency compared to ESCU.

Through this study, nanofluid with 0.24% volume concentration shows relatively

highest heat transfer coefficient between tube and working fluid and about 8% higher of that than water. Furthermore, it can see from the results that when the conductance is larger than 0.17 W/(mK) the increase of performance can be neglected, taking safety problems and economic problems into consideration, water is an ideal choose which has higher conductance than 0.17 and it will not corrode the copper tube and will not increase the cost significantly. Efficiency of solar collector will be increased about 4% with applying the water substituted by the air gap between copper fin and absorber tube. Besides, by using 50 solar collectors in a year, it can save about 615 kg coal which can release 1600 kg CO_2 and 5.3 kg SO_2, respectively. Through investigation on environmental and economic factors, the performance improvement of this study can slow down the Green house phenomena and help save a lot of money.

REFERENCE

Abdelrahman M., Fumeaux P., Suter P., 1979, Study of solid gas suspensions used for direct absorption of concentrated solar radiation, Solar Energy, Vol.22 pp.45-48.

Ali M., 2006, Heat loss through the piping of a large solar collector field,Energy, Vol.31, pp.2020-2035.

Azad E., 2008, Theoretical and experimental investigation of heat pipe solar collector, Experimental Thermal and Fluid Science, Vol.32, pp.1666-1672.

Beekley D.C., Mather G.R., 1975, Analysis and experimental tests of solar collector arrays based on evacuated tubular solar collectors, International Journal Proceedings of 1975 ISES Congress, Vol.20 (Ext. Abstract).

Duffie J.A., Bechman W.A., 1980, Solar engineering of thermal processes. John Wiley & Sons New York.

Dunn P., Reay D., 1982, Heat pipes, 3rd ed. Pergamon Press.

Dunn PwHottel H.C., Willier A., 1955, Evaluation of flat plate solar collector performance. Solar Energy, Vol. 2, pp. 74-104.

Fadar A.E., Mimet A., Azzabakh A., PérezGarcía M., Castaing J., 2009, Study of a

new solar adsorption refrigerator powered by a parabolic trough collector, Applied Thermal Engineering, Vol 29, pp. 1267-1270.

Fernandez-Garcia A., Zarza E., Valenzuela L., Perez M., 2010, Parabolic-trough solar collectors and their applications, Renewable and Sustainable Energy Reviews, Vol. 14, No. 7, pp. 1695-1721.

Frank P.I., David P.D., Theodore L.B., Adrienne S.L., 2005, Fundamentals of heat and mass transfer, 6th ed. John Wiley & Sons, Vol. 8, pp.481-533.

Garg H., 1975, Year-round performance studies on a built-in storage-type solar water heater at Jodhpur, India. Solar Energy, Vol 17, pp.167-172.

Han H., Kim J.T., Ahn H.T., 2008, A three-dimensional performance analysis of all-glass vacuum tubes with coaxial fluid conduit, International Communications in Heat and Mass Transfer, Vol.35, No.5, pp.589-596.

He W., Su Y.H., Riffat S.B., Hou J.X., Ji J., 2011, Parametrical analysis of the de-sign and performance of a solar heat pipe thermoelectric generator unit. Applied Energy, Vol.88, pp.5083-5089.

He W., Su Y.H., Wang Y.Q., Riffat S.B., Ji J,. 2012, A study on incorporation of thermoelectric modules with evacuated-tube heat-pipe solar collectors, Renew Energy, Vol.37, pp.142-149.

Hottel H, Woertz B., 1942, Performance of flat-plate solar-heat collectors, Trans ASME (Am Soc Mech Eng); (United States).

Hull J.R., 1986, Analysis of heat transfer factors for a heat pipe absorber array connected to a common manifold, Solar Energy, Vol.108, pp.11-16.

Kim J.T, Ahn H.T., Han H., Kim H.T., Chun W., 2007, The performance simulation of all glass vacuum tubes with coaxial fluid conduit. Int. Communications in Heat and Mass Transfer, Vol. 34, pp. 587-97.

Kim Y., Seo T., 2007, Thermal performances comparisons of the glass evacuated tube solar collectors with ‘shapes of absorber tube. Renewable Energy. Vol. 32, pp. 772-95.

Ma L., Zhen L., Zhang J., Liang R., 2010, Thermal performance analysis of the glass evacuated tube solar collector with U-tube, Building and Environment, Vol.45, pp.1959-1967.

Mahian O., Kianifar A., Kalogirou S.A., Pop I., Wongwises S., 2003, A review of the applications of nanofluids in solar energy, Int.J. Heat Mass Transf. Vol. 57, pp. 582-94.

Mohammadnejad M., Ghazvini M., Javadi F.S., Saidur R., 2011, Estimating the ex-ergy efficiency of engine using nanolubricants. Energy Education Science and Technology Part A: Energy Science and Research, Vol. 27, pp. 447-454.

Sani E., Barison S., Pagura C., Mercatelli L., Sansoni P., Fontani D., 2010, Carbon nanohorns-based nanofluids as direct sun light absorbers, Optics Express. Vol. 18, pp. 5179-5187.

Tian Q., 2006, Study on thermal efficiency and performance of U-tubular all-glass evacuated tube solar collector, Energy Engineering, Vol.6 pp.36-40.

Xu L., Wang Z.F., Yuan G.F., Ruan Y., 2012, A new dynamic test method for thermal performance of all-glass evacuated solar air collectors, Solar Energy, Vol.86, No.5, pp.1222-1231.

Yan S.Y., Tian R., Hou S., Zhang L.N., 2008, Analysis on unsteady state efficiency of glass evacuated solar collector with an inserted heat pipe, Journal of Engineering Thermophysics, Vol.29, No.2, pp.323-325 (in Chinese).

Wang Z, 2010, Prospectives for China's solar thermal power technology development, Energy, Vol 35, No.11, pp.4417-4420.

감사의 글

At the very moment of finishing this paper, I'd like to express my gratitude to Mr. Cho, my supervisor. Thanks for his encouragement, conscientiousness, edification and critics, I benefited a lot in the essay writing process. What's more, his guidance of some basic linguistic research methods not only helps me in linguistic study, but also lets me know the importance of responsibility and cautiousness. Secondly, I would also express my great thanks to all the members of REL. Without their help, it would be much harder for me to finish my study and this paper.

As first foreigner student here, I came here with curiosity and excitement even through I couldn't use this language and quite unfamiliar with this culture, I thought it really would be a hard time in Korea, time flies, the morning that 2 and half years ago are still in my mind, but with members and professor's help. We adapted the life here and now successfully graduated. Too many thanks and said also could not say, you forever on all my guide, forever always care about.

2014年 8月

신재생 에너지 실험실

동 역 걸